Journal of Hydrology 511 (2014) 589–593

Contents lists available at ScienceDirect

Journal of Hydrology

journal homepage: www.elsevier.com/locate/jhydrol

Human influence on changes in the distribution of land precipitation

Ramdane Alkama *

CNRM-GAME, Météo-France, CNRS, 31057 Toulouse, France
Joint Research Centre, European Commission, 27021 Ispra, VA, Italy

ARTICLE INFO

Article history:
Received 20 March 2013
Received in revised form 24 January 2014
Accepted 4 February 2014
Available online 12 February 2014
This manuscript was handled by Laurent Charlet, Editor-in-Chief, with the assistance of Martin Beniston, Associate Editor

Keywords:
Land precipitation change
Anthropogenic effect
CMIP5 experiments
Quantile mapping method

SUMMARY

The evolution of the distribution of observed land precipitation over 1901–2010 and 1979–2010 is analyzed and compared with 14 simulations from the CMIP5 climate models. Firstly, two different quantile-based mapping methods are used to bias-correct the simulated monthly land precipitation. The results show a very slight difference in mean annual values between the two methods. Secondly, the comparison between observed and simulated land precipitation suggests that anthropogenic forcing most likely caused the redistribution of the repartition of land precipitation, decreasing the extent of arid area (area with precipitation range between 50 and 300 mm/yr), and increasing the extent of area with a precipitation range between 450 and 900 mm/yr. However, the observed changes are larger than estimated from model simulations. The future RCP8.5 (2010–2100) simulations are also analyzed. Therefore, all 14 model simulations show the same trend pattern, only slightly different from that found over 1979–2010 but with reduced spread.

1. Introduction

Over the last decade, the human influence on global precipitation has been the subject of two categories of study. The first category did not detect any human influence on global precipitation, partly because changes in precipitation in different regions cancel each other out, thereby reducing the strength of the average global signal (Gillett et al., 2004; Lambert et al., 2004, 2005). However, in the second category, the decomposition of land precipitation on multiple latitudinal bounds allows the detection of human influence on land precipitation change (Zhang et al., 2007; Noake et al., 2012). This method has recently been used to detect the human influence on land evaporation (Douville et al., 2013).

These previous studies are all based on the precipitation simulated by an ensemble of climate models without using any bias correction method, despite the clear mismatch between the simulated and observed precipitation at local and regional scales (e.g. Li et al., 2010; Piani et al., 2010). This is further compounded by the inevitable model bias, the result of inadequate knowledge of key physical processes (e.g., cloud physics) and simplification of the natural heterogeneity of the climate system at finer spatial scales. On the other hand, averaging land precipitation along within latitudinal bins mixes different climates and, probably, different biases and thus complicates interpretation of trends. For instance, over the same latitude, the mean annual precipitation is less (more) than 50 (10,000) mm/yr over Tamanrasset in South Algeria (Tcherrapoundji North-East India).

Here, a new kind of detection study is proposed in which the bias of simulated land precipitation is corrected using a quantile-based mapping method. This detection method consists of comparing the observed and simulated change in the distribution of land precipitation. For this, two steps are required: (1) for each year, we divide the global land area into an ensemble of areas determined by bound of precipitation rate (for example, starting from 0 to 4000 mm/yr by an interval of 50 mm/yr); (2) we then construct the distribution of the trend of these surface areas according to the selected bounds of precipitation rate. This new method allows us to detect the human influence on changes in the distribution of land precipitation, in contrast with previous studies, (Zhang et al., 2007; Noake et al., 2012) which detected the human influence on latitudinal bounds.

2. Data sets

We used monthly precipitation observations over global land areas from the most recent version (Full Data Reanalysis V6 at 0.5° × 0.5° resolution) of the Global Precipitation Climatology Centre (GPCC, http://gpcc.dwd.de) product to analyze precipitation trends for the 1901–2010 and 1979–2010 periods. The latest version (Version 2.2 at 1° × 1° resolution) of the Global Precipitation

* Address: CNRM-GAME, Météo-France, CNRS, 31057 Toulouse, France. Tel.: +33 687855100.
E-mail address: ram.alkama@hotmail.fr

http://dx.doi.org/10.1016/j.jhydrol.2014.02.016
0022-1694

Climatology Project (GPCP) product is also used over the available period (1979–2010). The precipitation over Antarctica is not taken into account in this study. The GPCC is based on in situ monitoring, while GPCP is based on in situ and satellite monitoring. Few other precipitation datasets exist but the commonly used by the scientist are the two datasets used here which are considered as the best existing global precipitation product (e.g. Decharme and Douville, 2006), especially GPCC which is, for instance, used to create the WATCH Forcing Data (Weedon et al., 2011).

We compared observed trends to those simulated by fourteen climate models to determine whether observed changes over the two periods were caused by external influences on the climate system. The climate simulations were obtained from the multi-model data archive at PCMDI (http://pcmdi9.llnl.gov/). We considered two groups of historic simulations. One group (NAT) includes 12 simulations conducted using 12 models forced with natural external forcing only. A second group (ALL) includes 14 simulations conducted using 14 models forced with estimates of both historical anthropogenic and natural external forcing, including volcanic aerosols and solar irradiance changes. Future (RCP8.5 scenario) simulations of the same 14 models are also analyzed. The composition of each group is summarized in Table 1.

The GPCP product and the different modeled land precipitations products are bilinearly interpolated onto the same grid as the GPCC product, i.e. $0.5^\circ \times 0.5^\circ$ resolution.

3. Bias correction methods

Many quantile matching methods have been developed to reduce the bias of climate models (e.g. Panofsky and Brier, 1968; Li et al., 2010; Piani et al., 2010). Hence, the results could be method-dependent. For this reason, we chose to use two different methods to observe and test how the corrected values can be influenced by the choice of method.

The first method is the widely used quantile-based matching method that assumes stationarity and uses only the cumulative distribution functions (CDFs) of the model and observations for the baseline period (Panofsky and Brier, 1968). This method will hereafter be referred to as the "CLASSIC method". Put simply, to bias-correct model values for a projection period, we must first find the corresponding percentile values for these projection period points in the CDF of the model for the training period, and then locate the observed values for the same CDF values of the observations. These are the model values after bias correction.

The second method incorporates and adjusts the model CDF for the projection period on the basis of the difference between the model and observation CDFs for the training (baseline) period (Li et al., 2010). Thus, the method explicitly accounts for distribution changes for a given model between the projection and baseline periods. For a given percentile, we assume that the difference between the model and observed values during the training period also applies to the projection period, meaning that the adjustment function remains the same. However, the difference between the CDFs for the projection and training periods is also taken into account. This method will hereafter be referred to as the "DELTA method."

For more details concerning the two methods and their main differences, see Li et al. (2010). The GPCC product is used as the reference for the bias correction of the different model simulations. The training period chosen for this study is 1958–2001. In some cases several key limitations of using bias correction approaches can be noted (Ehret et al., 2012), especially when correcting future simulations. For this reason we chooses to include both studies with and without bias correction in the present work.

Table 1
Summary of the different model simulations used in this study.

Models	Historic 1901–2010		Future 2010–2100
	All	Nat	RCP 8.5
BCC-CSM1-1	×	×	×
CanESM2	×	×	×
CCSM4	×	×	×
CNRM-CM5	×	×	×
CSIRO-Mk3-6-0	×	×	×
FGOALS-g2	×	×	×
GFDL-ESM2M	×	×	×
GISS-E2-R	×	×	×
INMCM4	×		×
IPSL-CM5A-LR	×	×	×
MIROC5	×		×
MIROC-ESM		×	
MPI-ESM-LR	×		×
MRI-CGCM3	×	×	×
NorESM1-M	×	×	×

4. Results

Fig. 1 represents precipitation over the world's 18 largest river basins as observed (GPCC), simulated (CNRM-CM5), and bias-corrected by the two different methods (CLASSIC and DELTA). In this figure, we choose to show only the results of the historical (ALL) and future (RCP 8.5) CNRM-CM5 simulation model, but the conclusions are the same for the other 13 model simulations, i.e. (1) the different biases are reduced when using the quantile-based matching methods over all 18 river basins; (2) the mean annual difference between the CLASSIC and DELTA correction methods is very slight. This implies that the choice of method does not alter the result of the detection method. Whereas, in order to use the banding approach, the simulated precipitation over each band has to be close to observations, otherwise we will compare two geographically different area.

Throughout this paper, trends and *P*-values are computed using Student's *t*-test, assuming that the mean annual precipitation at year N and year N + 1 are independent. One can note that a *P*-value smaller than 0.01 indicates a trend that is significant at the 0.99 level. Fig. 2 (top) shows the distribution of the trend of land areas (km^2/yr) by the bounds of precipitation rate (GPCC) of 50 mm/yr (from 0 to 4000 mm/yr) over 1901–2010 and (bottom) their corresponding *P*-value. This methodology allows us to identify the bounds of observed precipitation where the area changes significantly, i.e. *P*-value smaller than 0.01. According to Fig. 2, the areas receiving less than 50 mm/yr (hyper arid area) and between 550–700 mm/yr increased significantly, by about 30,000 km^2/yr and 15,000 km^2/yr, respectively. This is compensated by the significant decrease of about 55,000 km^2/yr of the surface area receiving precipitation between 50 and 250 mm/yr (arid area).

Fig. 3 represents the cumulative distribution functions of the probability of land surface area averaged over 15-year time periods from 1905 to 2010, with the horizontal axis representing precipitation (from 0 to 4000 mm/yr). This figure shows a clear rightward shift of the CDFs over time, especially since 1980, when this shift becomes more apparent and coincides with the acceleration of human greenhouse gas emission. Thus, the human influence could be suspected as the driver of the observed change in the repartition of land precipitation.

To test how humans impact this distribution, trends in observed and simulated (ALL and NAT historical simulations) surface areas were computed and compared. We analyzed trends in the distribution of the average annual surface areas by bounds of 50 mm/yr of precipitation. Fig. 4 shows that the spread is reduced in model-simulated trends is reduced and the multi-model means are closer

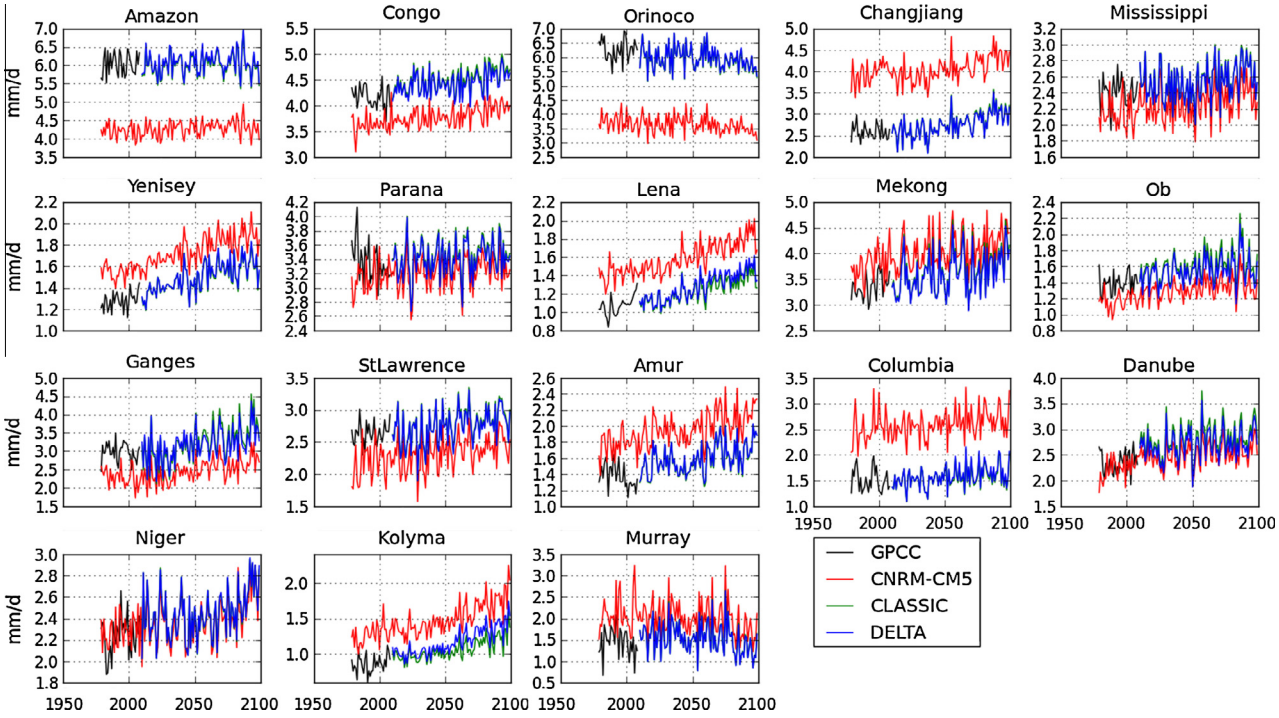

Fig. 1. Comparison between observed (GPCC in black), simulated (CNRM-CM5 in red) and bias corrected (by CLASSIC and DELTA, in green and blue, respectively) yearly average precipitation over the 18 largest river basins.

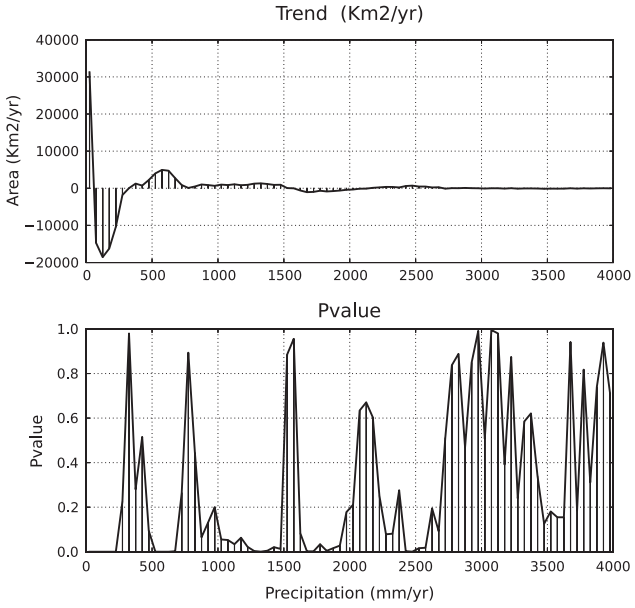

Fig. 2. (Top) Represents the distribution of the trend of land surface area (km^2/yr) by bounds of precipitation rate (GPCC) of 50 mm/yr (from 0 to 4000 mm/yr) over 1901–2010 and (bottom) their corresponding *P*-values.

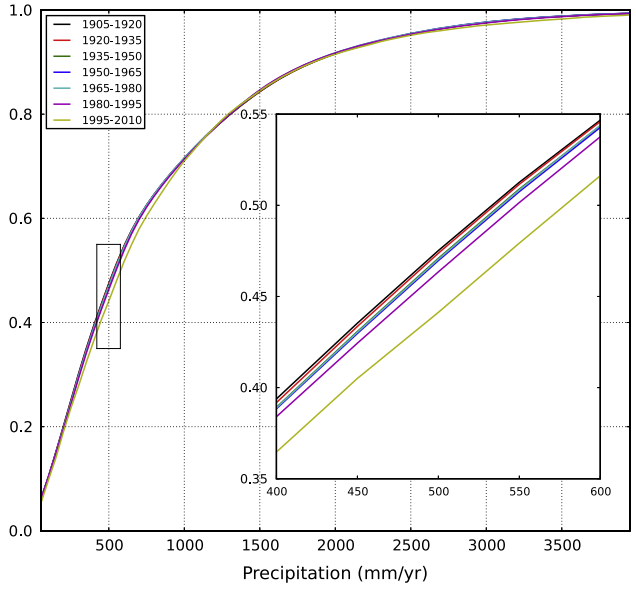

Fig. 3. Cumulative distribution functions, where the horizontal axis represents precipitation (from 0 to 4000 mm/yr). The vertical axis is a probability of land surface area averaged by 15-year time periods from 1905 to 2010.

to the observations in the case of bias-corrected precipitations. Linear annual surface trends from observations and the average of multiple model simulations for 1901–2010 (Fig. 4(b)) exhibit important areas of consistency in the spatial distribution change by bounds of precipitation rate. Both observations and models show that the surface increased for the 400–1500 mm/yr precipitation range and decreased for the 50–400 mm/yr range. We note an important difference, however: observations suggest an upward trend in the hyper-arid areas (less than 50 mm/yr), while the mean ALL simulation shows a slight downward trend. We also note that the observed changes are larger than estimated by model simulations. This is also true when using the average latitudinal method (Zhang et al., 2007; Noake et al., 2012). We obtained relatively similar results for the recent 1979–2010 trends, (Fig. 4(e)) which shows slight differences in the surface trend in the two observed (GPCC and GPCP) data sets. Both observations and models show that the surface exhibits a large increase for the precipitation range of 600–1000 mm/yr and a decrease for the range of 100–400 mm/yr. The trends in the surface of hyper-arid areas still contrasted.

When only natural effects (NAT) are taken into account, the annual surface trends from the average of multiple model

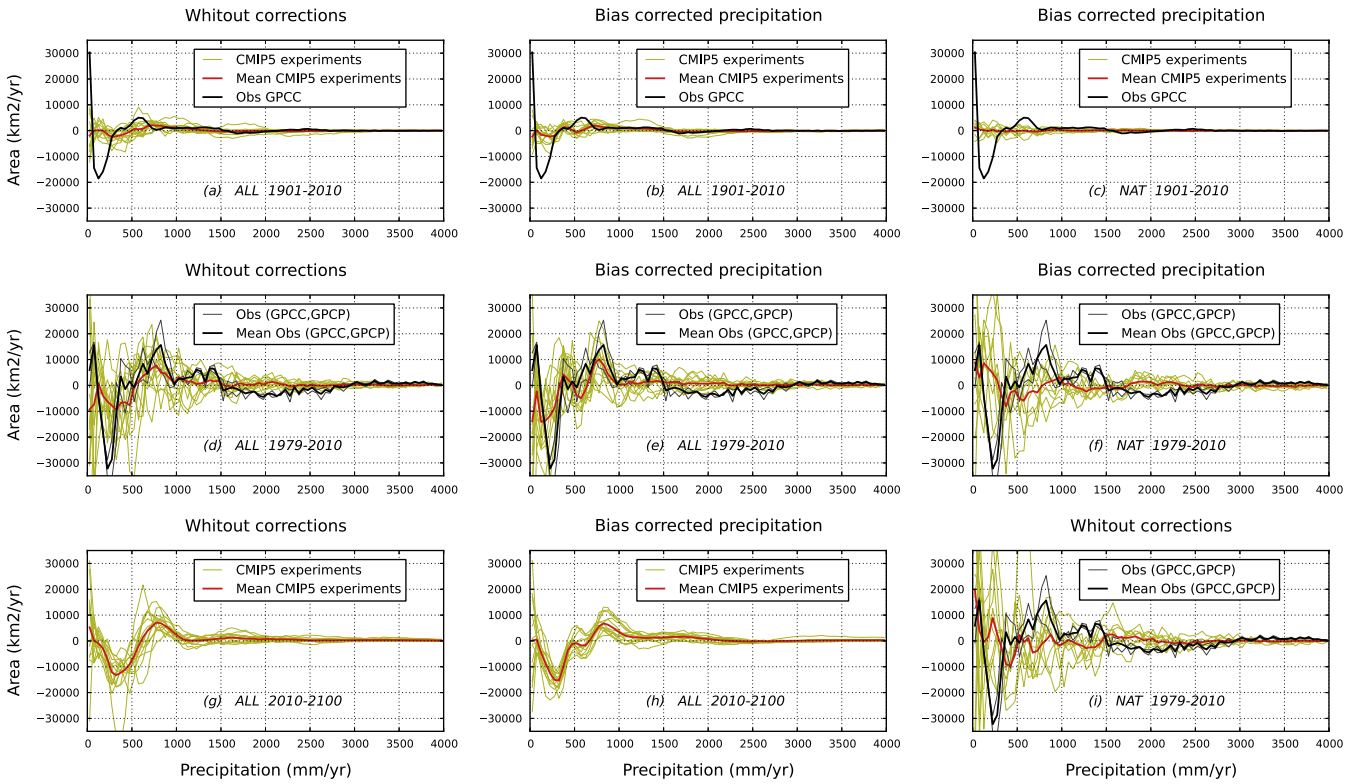

Fig. 4. Comparison between observations (in black) and simulations (in orange with their averaged value in red) of trends in the distribution of the average annual surface areas by bounds of 50 mm/yr of precipitation. The first (second and third) columns show the results of ALL (ALL and NAT respectively) without (with) bias correction method.

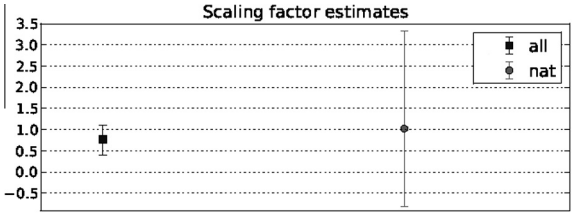

Fig. 5. Attribution analysis based on global average time series over 1979–2010. The scaling factors estimates are shown for the average of the 14 climate models used in this study, in two forcing analysis All (square) and Nat (circle). The results shown her are based on the regularised optimal fingerprint method (Ribes et al., 2013).

simulations do not show any trend over 1901–2010 (Fig. 4(c)) and a slight or generally opposite trend with observations over 1979–2010 (Fig. 4(f)). This means that the change in the spatial distribution of land precipitation cannot be explained without invoking anthropogenic radiative forcings. Contrary to the historical periods, which show large uncertainty trends between different models, all of the 14 future 2010–2100 simulations exhibit the same trend pattern (Fig. 4(h)), with increased surface area for the 700–2000 mm/yr precipitation range, and decreased surface area for the 100–500 mm/yr range.

5. Discussion and conclusions

The bias of the simulated land precipitation was adjusted using two different quantile matching methods. The results show that the low frequency (yearly) of corrected precipitation is not sensitive to the choice of quantile matching method. Moreover, the quantile matching method considerably improves the distribution of trends in average annual surface area by bounds of regions of precipitation. This improvement is essentially explained by the correction of the mean annual values. Indeed, when comparing the precipitation bound area between observations and simulations without bias correction method, we allow comparing two geographically different area. The uncertainty between the different simulations is also reduced, but still large, except over the future period 2010–2100 under the RCP8.5 scenario, in which all 14 models exhibit the same distribution of trend patterns.

An investigation was carried out to determine whether observations show an influence on the anthropogenic forcing by analyzing the 1901–2010 and 1979–2010 periods of land precipitation change, and an original method was developed. The results show that anthropogenic forcing contributed significantly to the observed changes and that these changes cannot be explained by internal variability and natural forcing. Indeed, by using the regularised optimal fingerprinting method (Ribes et al., 2013) to simulated both All (natural and anthropic) and only Nat (natural) precipitation, see Fig. 5, we detect change (i.e. scaling factor inconsistent with zero and consistent with one) in the distribution of land precipitation over 1979–2010, and this changing cannot be explain by the natural effect only because of scaling factor is consistent with zero in the natural simulations.

The Zhang et al. (2007) method has the advantage of separating the precipitation of cold high latitude from the warm tropics; however, at the same latitudinal bound, this method did not distinguish between the arid and temperate regions. The original method proposed here separates the regions by bounds of precipitation range. This means that the arid and temperate regions are separated, but the cold and warm areas are not differentiated. The alternative would be to combine the two methods by, for example, using the proposed method over three latitudinal bounds 90S-30S, 30S-30N, 30N-90N. Using this wetness band approach means that the bands will move in time and space, and be subject

to different climate processes in the future and past; in addition this spatiotemporal movement may make the results harder to apply to societal impacts.

Acknowledgements

The author acknowledges the use of precipitation data from the GPCC and GPCP groups, as well as the modeling groups that contributed to the data archive at PCMDI. I also thank A. Ribes who provide the fingerprint tools used in this study, and all of C. Delire, B. Decharme and anonymous reviewers for their constructive comments. This work was supported by CLASSIQUE ANR French project and the climate risk management unit of Joint Research Centre (JRC).

References

Decharme, Douville, 2006. Uncertainties in the GSWP-2 precipitation forcing and their impacts on regional and global hydrological simulations. Clim. Dyn. 27 (7–8), 695–713.

Douville, H., Decharme, B., Ribes, A., Alkama, R., Sheffield, J., 2013. Anthropogenic influence on multi-decadal changes in reconstructed global evapotranspiration. Nature Climate Change (3), 59–62. http://dx.doi.org/10.1038/nclimate1632.

Ehret, U., Zehe, E., Wulfmeyer, V., Warrach-Sagi, K., Liebert, J., 2012. HESS opinions should we apply bias correction to global and regional climate model data?ss. Hydrol. Earth Syst. Sci. 16, 3391–3404. http://dx.doi.org/10.5194/hess-16-3391-2012.

Gillett, N.P., Weaver, A.J., Zwiers, F.W., Wehner, M.F., 2004. Detection of volcanic influence on global precipitation. Geophys. Res. Lett. 31 (L12217), 2004G. http://dx.doi.org/10.1029/L020044.

Lambert, F.H., Stott, P.A., Allen, M.R., Palmer, M.A., 2004. Detection and attribution of changes in 20th century land precipitation. Geophys. Res. Lett. 31, L10203. http://dx.doi.org/10.1029/2004GL019545.

Lambert, F.H., Gillett, N.P., Stone, D.A., Huntingford, C., 2005. Attribution studies of observed land precipitation changes with nine coupled models. Geophys. Res. Lett. 32, L18704. http://dx.doi.org/10.1029/2005GL023654.

Li, H., Sheffield, J., Wood, E.F., 2010. Bias correction of monthly precipitation and temperature fields from intergovernmental panel on climate change AR4 models using equidistant quantile matching. J. Geophys. Res. 115, D10101. http://dx.doi.org/10.1029/2009JD012882.

Noake, K., Polson, D., Hegerl, G., Zhang, X., 2012. Changes in seasonal land precipitation during the latter twentieth-century. Geophys. Res. Lett. 39, L03706. http://dx.doi.org/10.1029/2011GL050405.

Panofsky, H.A., Brier, G.W., 1968. Some Application of Statistics to Meteorology. Pa. State Univ., University Park, Pa, pp. 224.

Piani, C., Haerter, J.O., Coppola, E., 2010. Statistical bias correction for daily precipitation in regional climate models over Europe. Theor. Appl. Climatol. 99, 187–192. http://dx.doi.org/10.1007/s00704-009-0134-9.

Ribes, A., Terray, L., Planton, S., 2013. Application of regularised optimal fingerprinting to attribution. part i: method, properties and idealised analysis. Clim. Dyn. 41 (11–12), 2817–2836.

Zhang, X., Zwiers, F., Hegerl, G., Lambert, F., Gillett, N., Solomon, S., Stott, P., Nozawa, T., 2007. Detection of human influence on twentieth-century precipitation trends. Nature 448 (7152), 461–465.

Weedon, G.P. et al., 2011. Creation of the WATCH Forcing data and its use to assess global and regional reference crop evaporation over land during the twentieth century. J. Hydrometeor. 12, 823–848. http://dx.doi.org/10.1175/2011JHM1369.1.